

Natural Killer Cells Are Essential for the Ability of BRAF Inhibitors to Control BRAF^{V600E}-Mutant Metastatic Melanoma

Lucas Ferrari de Andrade^{1,2}, Shin F. Ngiew², Kimberley Stannard², Sylvie Rusakiewicz^{3,4,5}, Murugan Kalimuthu⁶, Kum Kum Khanna⁶, Siok-Keen Tey⁷, Kazuyoshi Takeda⁸, Laurence Zitvogel^{3,4,9,10}, Ludovic Martinet², and Mark J. Smyth^{2,11}

Abstract

BRAF^{V600E} is a major oncogenic mutation found in approximately 50% of human melanoma that confers constitutive activation of the MAPK pathway and increased melanoma growth. Inhibition of BRAF^{V600E} by oncogene targeting therapy increases overall survival of patients with melanoma, but is unable to produce many durable responses. Adaptive drug resistance remains the main limitation to BRAF^{V600E} inhibitor clinical efficacy and immune-based strategies could be useful to overcome disease relapse. Tumor microenvironment greatly differs between visceral metastasis and primary cutaneous melanoma, and the mechanisms involved in the antimetastatic efficacy of BRAF^{V600E} inhibitors remain to be determined. To address this question, we developed a metastatic BRAF^{V600E}-mutant melanoma cell line and demonstrated that the antimetastatic properties of BRAF inhibitor PLX4720 (a research analogue of vemurafenib) require host natural killer (NK) cells and perforin. Indeed, PLX4720 not only directly limited BRAF^{V600E}-induced tumor cell proliferation, but also affected NK cell functions. We showed that PLX4720 increases the phosphorylation of ERK1/2, CD69 expression, and proliferation of mouse NK cells *in vitro*. NK cell frequencies were significantly enhanced by PLX4720 specifically in the lungs of mice with BRAF^{V600E} lung metastases. Furthermore, PLX4720 also increased human NK cell pERK1/2, CD69 expression, and IFN γ release in the context of anti-NKp30 and IL2 stimulation. Overall, this study supports the idea that additional NK cell-based immunotherapy (by checkpoint blockade or agonists or cytokines) may combine well with BRAF^{V600E} inhibitor therapy to promote more durable responses in melanoma. *Cancer Res*; 74(24): 7298–308. ©2014 AACR.

Introduction

Metastatic melanoma is a skin cancer with increasing incidence rate and poor prognosis. The mean 5-year relative survival rate for metastatic melanoma is only 16% (1). Until

recently, the therapeutic options for patients with advanced-stage metastatic melanoma were very limited and remained largely ineffective in improving patient's survival (1). The identification of activating point mutations of the *BRAF* gene has been a major breakthrough in the management of metastatic melanoma (2). Valine to glutamic acid substitution at codon 600 (BRAF^{V600E}) is the most common mutation present in *BRAF* gene and is approximately found in 50% of all melanoma cases (3). BRAF^{V600E} has been shown to trigger constitutive activation of the MAPK pathway, resulting in increased cell proliferation and invasiveness (2). The large proportion of patients bearing BRAF^{V600E} mutations provided a strong rationale for the development of small-molecule-based BRAF^{V600E}-selective inhibitors. Vemurafenib (PLX4032), and its research analogue PLX4720, are ATP-competitive inhibitors for BRAF^{V600E} shown to reduce the kinase activity of this protein, consequently inhibiting the MAPK pathway and cell proliferation of BRAF^{V600E}-mutated melanoma (4, 5). Vemurafenib demonstrated improved overall and progression-free survival rates in most patients with previously untreated BRAF^{V600E} melanoma (3, 6) and was approved in 2011 by the U.S. FDA in the treatment of late-stage or unresectable melanoma (FDA Reference ID: 3001518). However, complete and durable remissions were rarely observed and progression-free

¹Laboratório de Pesquisa em Células Inflamatórias e Neoplásicas Group, Universidade Federal do Paraná, Curitiba, Paraná, Brazil. ²Immunology in Cancer and Infection Laboratory, QIMR Berghofer Medical Research Institute, Herston, Queensland, Australia. ³Gustave Roussy Cancer Campus, Villejuif, France. ⁴INSERM U1015, Villejuif, France. ⁵Center of Clinical Investigations in Biotherapies of Cancer (CICBT) 1428, Villejuif, France. ⁶Signal Transduction Laboratory, QIMR Berghofer Medical Research Institute, Herston, Queensland, Australia. ⁷Bone Marrow Transplant Laboratory, QIMR Berghofer Medical Research Institute, Herston, Queensland, Australia. ⁸Department of Immunology, Juntendo University School of Medicine, Hongo, Bunkyo-ku, Tokyo, Japan. ⁹Université Paris Sud-XI, Faculté de Médecine, Le Kremlin Bicêtre, France. ¹⁰Department of Medical Oncology, IGR, Villejuif, France. ¹¹School of Medicine, University of Queensland, Herston, Queensland, Australia.

Note: Supplementary data for this article are available at Cancer Research Online (<http://cancerres.aacrjournals.org/>).

Corresponding Author: Mark J. Smyth, Immunology in Cancer and Infection Laboratory, QIMR Berghofer Medical Research Institute, 300 Herston Road, Herston 4006, Queensland, Australia. Phone: 61-7-8345-3957; Fax: 61-7-3362-0111; E-mail: mark.smyth@qimrberghofer.edu.au

doi: 10.1158/0008-5472.CAN-14-1339

©2014 American Association for Cancer Research.

survival did not exceed 5 to 7 months upon treatment with BRAF inhibitors (7). Drug resistance remains to date a major factor that limits BRAF^{V600E} inhibitor clinical efficacy and the discovery of strategies overcoming adaptive resistance may have a huge impact on a patient's clinical outcome (8, 9).

BRAF^{V600E} mutation contributes to melanoma immune escape (10) and accumulating evidence indicates that the efficacy of BRAF inhibitors relies on the activation of immune components against cancer cells (11–14). BRAF inhibition was associated with a decreased production of immunosuppressive soluble factors such as IL10, VEGF, and IL6 (12, 14, 15). An enhanced expression of melanoma-associated antigens together with an increased infiltration of CD8⁺ T lymphocytes was also observed in metastases of patients receiving BRAF inhibitors (12–14, 16). Using resistant variants of BraF^{V600E}-driven mouse melanoma and melanoma-prone mice, our group recently demonstrated that combination therapy between PLX4720 and anti-CCL2 or agonistic anti-CD137 antibodies had significant antitumor activity, suggesting that immune-based therapy represents a promising strategy to overcome BRAF inhibitor drug resistance (11, 17).

Tumor microenvironment differs greatly between visceral metastases and primary cutaneous melanoma and may directly affect antitumor immune reactions and the efficacy of BRAF^{V600E} inhibitors (18, 19). A better understanding of the antimetastatic effect of BRAF inhibitors is therefore required. In this study, using the first described mouse model for metastatic BRAF^{V600E} melanoma, we establish that natural killer (NK) cells are critical for the therapeutic effect of PLX4720 through a perforin-dependent pathway. We show that PLX4720 treatment, in the context of IL2, directly enhances mouse NK cell ERK1/2 phosphorylation, proliferation, and CD69 expression and human NK cell ERK1/2 phosphorylation, CD69 expression and IFN γ release post Nkp30 ligation. Finally, we demonstrate that treatment with a low dose of IL2 improves the antimetastatic efficacy of PLX4720 providing a strong rationale for combining NK cell stimulatory agents and BRAF inhibitors in metastatic melanoma.

Materials and Methods

Cell lines

The BRAF^{V600E} SMIWT1 melanoma cell line has already been described (11). The LWT1 cell line was derived from SMIWT1 by the intravenous injection of 5×10^5 SMIWT1 into C57BL/6 wild type (WT) mice (Fig. 1). Both SMIWT1 and LWT1 cell lines were maintained in complete RPMI-1640 with 10% heat-inactivated FCS, 2 mmol/L glutamax, 100 U/mL penicillin, and 100 μ g/mL streptomycin. The genotyping for BRAF^{V600E} was achieved as previously described (20). B16F10 cells were sourced from ATCC, cultivated in complete DMEM supplemented as above. The original B16F10 cells were short tandem repeat DNA profiled, grown to bulk, and were never passaged for more than 2 weeks. They were routinely tested for mycoplasma by MycoAlert mycoplasma detection kit (Lonza, catalog number LT07-318).

Mice

C57BL/6 WT mice were purchased either from Animal Resources Centre or Walter and Eliza Hall Institute of Medical Research (Parkville, Australia) and maintained at QIMR Berghofer Medical Research Institute (QIMR, Herston, Australia). C57BL/6 *Cd226*^{-/-}, *Ifng*^{-/-}, and *Pfp*^{-/-} mice have been previously described (11) and were bred, genotyped, and maintained at the QIMR. Seven- to 12-week-old male mice were used according to the QIMR animal ethics committee.

In vitro treatment of LWT1 and B16F10

The IC₅₀ of the cell lines were determined by Alamar Blue (Invitrogen, catalog number DAL1025) assay according to the manufacturer's instructions. MHC class I, Rae-1, and CD155 expression were analyzed on LWT1 or B16F10 cells after 24 hours in the presence of PLX4720 (10 μ mol/L) or an equivalent amount of DMSO. Cells were then incubated with Fc blocking buffer (2.4G2 antibody) and the following fluorescence conjugated mAbs: anti-mouse- CD155 (4.42.3), Rae-1 (186107), and relevant IgG isotype controls, all from Biolegend or R&D Systems. MHC class I was detected by incubation with biotinylated anti-mouse H2K^b (AF6-88.5) or H2D^b (28-14-8), with subsequent incubation with Allophycocyanin-conjugated streptavidin, all from BD Biosciences (catalog number 554067). All antibodies were diluted in 0.5% FCS 2 mmol/L EDTA PBS. Samples were acquired on a LSR IV Fortessa Flow Cytometer (BD Biosciences). Data were analyzed on FlowJo V10 (Treestar).

Western blotting

LWT1 or B16F10 cells were treated with 2.5, 5.0, or 10.0 μ mol/L of PLX4720 or equivalent amount of DMSO. Purified human and mouse NK cells were cultivated with 1 μ mol/L of PLX4720 or DMSO in complete RPMI supplemented with 300 U/mL IL2. After 24 hours, cells were harvested and resuspended in RIPA lysis buffer with protease inhibitors (Roche Diagnostics GmbH), 1 mmol/L sodium orthovanadate (Sigma), and 10 mmol/L sodium fluoride. Cells were then lysed by passing them through a 25-gauge needle 10 times and centrifuged at 13,200 rpm/4°C for 20 minutes to remove cell debris. Protein concentration was determined using the bicinchoninic acid protein assay reagent (Pierce, Thermo Fisher Scientific). Each protein sample (30 μ g) was resolved on SDS-polyacrylamide gels and transferred to a PROTRAN BA 83 nitrocellulose membrane (Whatman Schleicher & Schuell; Sigma). Immunodetections were performed using anti-pERK1/2Thr202/204 (D13.14.4, #4370) and ERK1/2 (137F5, #4695, Cell Signaling Technology), anti-c-MYC (Y69, #1472-1, Abcam) rabbit polyclonal antibodies were used in conjunction with an horseradish peroxidase-conjugated anti-rabbit secondary antibody (Amersham, GE Healthcare). Equal loading was assessed using β -actin (Sigma) mouse monoclonal primary antibodies. The Super Signal chemiluminescent system (Pierce, Thermo Fisher Scientific) or ECL-plus (Amersham) was used for detection. Quantification of protein-band intensities by densitometric analysis was performed using NIH ImageJ software (NIH, Bethesda, MD).

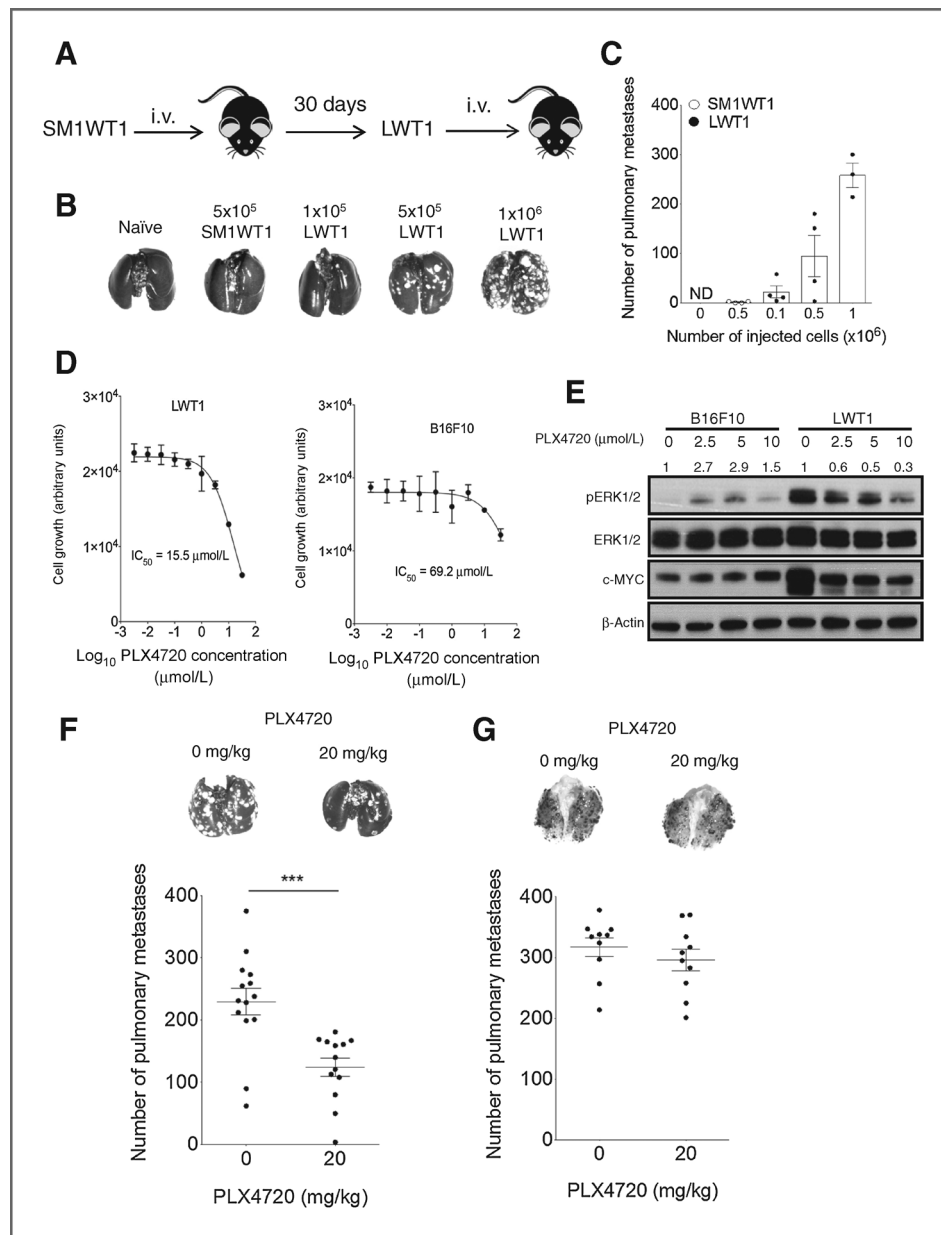


Figure 1. LWT1 is a model of metastatic BRAF^{V600E} melanoma sensitive to PLX4720 inhibition. A, metastatic BRAF^{V600E}-mutant cell line LWT1 was generated by intravenous injection of 5×10^5 SM1WT1 cells into C57BL/6 WT mice. After 30 days, the lungs with tumor nodules were meshed through a 70- μ m cell strainer and cultured as described in Materials and Methods. B and C, the indicated doses of LWT1 or SM1WT1 parental cell lines were injected intravenously in WT mice. After 14 days, lungs were harvested, perfused with India ink, and the number of metastases was counted under a microscope. B, representative pictures of lungs from each group of mice. C, graph representing the mean \pm SEM number of lung metastases in the indicated group of mice. Each symbol represents one individual mouse. ND, not detected. D and E, LWT1 or B16F10 melanoma cells were treated *in vitro* with the indicated doses of PLX4720 or equivalent amount of DMSO. D, graph showing the mean \pm SEM proliferation (Alamar Blue assay) of the LWT1 and B16F10 cell lines after 48 hours of culture with the indicated dose of PLX4720. Data are representative of three independent experiments. E, representative Western blot analysis with the indicated antibodies. Data are representative of three independent experiments. Fold increase in pERK1/2 relative to no PLX 4720 control is recorded above the lane. F and G, 5×10^5 LWT1 (F) or 2×10^5 B16F10 (G) were injected i.v. in C57BL/6 WT mice. Mice were treated with 20 mg/kg or equivalent amount of DMSO daily from day 1 to 7. After 14 days, lungs were harvested and representative picture of lungs from each group of mice and graph representing the mean \pm SEM number of lung metastases in the indicated groups of mice are shown. Pooled data from two independent experiments are shown. Each symbol representing one individual mouse. ***, $P < 0.001$ Mann-Whitney test.

Transplant model and treatments

Pulmonary metastasis assays were performed by tail vein injection of 5×10^5 LWT1 cells or 2×10^5 B16F10 cells. PLX4720 (20 mg/kg) or equivalent amount of DMSO was given daily

from day 1 to day 7 relative to tumor cell inoculation by i.p. injections. To examine IL2 immunotherapy of metastases, some groups of mice received either PBS or recombinant IL2 (10,000 or 100,000 U, Chiron Corporation) from day 1 to 5.

Antibody depletions were performed by i.p. injections of 100 µg of control rat IgG (HRPN – BioExcell), anti-CD4 (GK1.5 – BioExcell), anti-CD8β (53.5.8 – BioExcell), anti-NK1.1 (PK136 – BioExcell), anti-IFNγ (H22 – prepared in house), anti-NKG2D (C7 – prepared in house), or anti-asialo(as)GM1 (Wako Chemicals) on days –1, 0, and 7, relative to tumor challenge. The *in vivo* immune modulatory effects of PLX4720 on spleen NK cells were tested by daily treatment with 20 mg/kg of PLX4720 or an equivalent amount of DMSO for 3 days followed by euthanasia and analysis of NK cells from spleens by flow cytometry. To visualize the LWT1 metastasis, lungs were intratracheally perfused with 30% India Ink PBS, followed by PBS wash and 24-hour incubation with Fekete's Solution. Lung photographs and metastasis counts were both performed with a Nikon SMZ745T microscope and NIS-Elements (F.4) software.

Cells preparation and flow cytometry

Spleens were meshed, filtered at 70 µm, and washed in PBS. Red blood cells were lysed by ACK buffer incubation for 1 minute. Single-cell suspensions were incubated for 15 minutes in Fc blocking buffer (2.4G2 antibody) and stained with the following fluorescence-conjugated mAbs, all diluted at 0.5% FCS 2 mmol/L EDTA PBS: anti-mouse- CD3ε (145-2C11), TCRβ (H57-597), and NK1.1 (PK136). All mAbs were purchased from Biologend or eBioscience. Samples were acquired on a LSR IV Fortessa Flow Cytometer (BD Biosciences). Data were analyzed on FlowJo V10 (Treestar).

In vitro activation of mouse and human NK cells

C57BL/6 spleen NK cells were purified by flow cytometry (Beckman Coulter MoFlo High Speed Cell Sorting) after staining with anti-CD3ε (145-2C11) and NK1.1 (PK136). NK cells were stained with 1 µmol/L Cell Trace Violet (Invitrogen) for 10 minutes at 37°C followed by FCS and PBS wash. Human peripheral blood mononuclear cells (PBMC) were prepared on a Ficoll–Paque density gradient (Amersham Biosciences AB) by centrifugation (800 × *g*, 30 minutes at room temperature) and human CD3[–]CD56⁺ NK cells were negatively selected by magnetically activated cell sorting (NK cell isolation kit II, Miltenyi Biotec) according to the manufacturer's instructions.

Mouse or human NK cells were then cultured with the indicated concentrations of PLX4720 or an equivalent amount of DMSO in complete RPMI-1640 supplemented with 300 U/mL of human recombinant IL2. The analysis of ERK phosphorylation was performed after 24 hours in both species. Mouse NK cell activation and proliferation were assessed by flow cytometry by CD69 staining (H1.2F3) and Cell Trace Violet dilution after 3 days of cultures. Human NK cell activation was analyzed by CD69 expression after 6 days of culture.

In some experiments, purified NK cells (from 9 different donors) were cultured overnight (20 hours) in complete medium (RPMI 10% plus Human AB serum, 1% penicillin/streptomycin, 2 mmol/L glutamine, 2 mmol/L sodium pyruvate) with DMSO, PLX (0.3–3.0 µmol/L) with or without IL2 (300 U/mL). NK cells were recovered, counted, and plated (5 × 10⁴/well) in a

96-well MAXISORB cross-linking plate (Nunc) precoated with 2.5 µg/mL anti-NKp30 (clone 210847, R&D Systems) or the IgG2a isotype control. NK cells were incubated at 37°C for an additional 20 hours and the supernatants were harvested and IFNγ measured by ELISA (BD Biosciences).

⁵¹Cr release cytotoxicity assay

NK cells were stimulated with 10 ng/mL of IL15/IL15R complex (eBioscience; #14-8152-80) for 48 hours in complete RPMI and used as effector cells. LWT1 or B16F10 cells were treated with 10 µmol/L of PLX4720 or equivalent amount of DMSO for 24 hours and used as target cells. The target cells were incubated with ⁵¹Cr for 60 minutes, washed in PBS, and 1,000 cells dispensed in 96-well V bottom plates. Effector cells were plated at an effector:target ratio of 1:1, 5:1, and 10:1, and incubated at 37°C for 4 hours. When indicated rat IgG (HRPN – BioExcell, 10 µg/mL), or anti-CD226 (480.1 – BioExcell, 10 µg/mL) was used in the assay. ⁵¹Cr release in the supernatant was determined by reading on a Wallac 1470 WIZARD Gamma Counter and the % of killing calculated by the following equation: % specific killing = (sample cpm – spontaneous release)/(maximum release – spontaneous release) × 100.

Statistical analysis

Statistical analysis was achieved using GraphPad Prism 6 software. Unpaired Mann–Whitney test or Student *t* test was used for comparison between groups with statistical significance when *P* values were below or equal to 0.05 (*), 0.01 (**), or 0.001 (***)

Results

LWT1 is a model of metastatic BRAF^{V600E} melanoma sensitive to PLX4720 inhibition

In the absence of immune-competent BRAF^{V600E} melanoma models, the mechanisms involved in antimetastatic efficacy of BRAF^{V600E}-specific inhibitor PLX4720 remain unknown. We therefore derived an experimental metastatic cell line from the previously described BRAF^{V600E} SM1WT1 melanoma (11, 20) by intravenous passage through the lungs of a wild-type (WT) mouse (Fig. 1A). This metastatic melanoma cell line, termed LWT1, induced in 2 weeks the consistent formation of metastatic colonies restricted to the lungs in a dose-dependent manner, whereas the injection of an equal number of parental cell line SM1WT1 did not (Fig. 1B and C). Consistent with previous results obtained with the parental cell line SM1WT1 (11), we found that PLX4720 had modest activity against LWT1 (somewhat PLX4720 resistant; IC₅₀ = 15.5 µmol/L), whereas PLX4720 had little detectable effect on BRAF^{wt} melanoma cell line B16F10 (IC₅₀ = 69.2 µmol/L; Fig. 1D). ERK1/2 was constitutively phosphorylated in the LWT1 BRAF^{V600E} cell line and treatment with PLX4720 for 24 hours produced a dose-dependent reduction in the phosphorylation of ERK1/2 (Fig. 1E). This was associated with a decrease in c-Myc expression, a downstream target of ERK1/2 involved in cell proliferation (4), confirming the inhibition of the MAPK pathway by PLX4720 (Fig. 1E). In

contrast, the basal level of ERK1/2 phosphorylation was very low in BRAF^{WT} B16F10 tumors but low concentrations of PLX4720 slightly increased the phosphorylation of ERK1/2 and had no impact on c-Myc expression (Fig. 1E). These data confirm the findings of previous reports showing that PLX4720 promotes the phosphorylation of ERK in BRAF^{WT} melanoma cells (21, 22). We then tested the antimetastatic effect of PLX4720 *in vivo* and it was able to reduce the quantity of pulmonary metastatic foci of LWT1 by approximately 50% (Fig. 1F), while it did not affect the number of B16F10 metastases (Fig. 1G). PLX4720 was superior to either anti-CTLA-4 or anti-PD-1 treatment alone and enabled enhanced survival in this model (Supplementary Fig. S1). These results show in a metastatic context that PLX4720 has specific antimetastatic effects against BRAF^{V600E} melanoma cell lines.

PLX4720 control of pulmonary LWT1 metastasis is NK cell dependent

Given the accumulating evidence showing the ability of BRAF inhibitors to modulate antimelanoma immune reactions, we analyzed the role of immune components in PLX4720 antimetastatic properties *in vivo*. PLX4720 greatly reduced the number of metastases in the lungs of Ig-treated mice as compared with DMSO-treated group (Fig. 2A and B). Similar reduction with PLX4720 was observed in mice depleted with both CD4 and CD8 mAbs (Fig. 2B). In contrast, we found that this drug had no detectable antimetastatic effect in NK cell-depleted mice (Fig. 2A and B). The role of NK cells in PLX4720 efficacy was subsequently validated using another antibody to deplete NK cells (anti-NK1.1; PK136; Fig. 2B). The antimetastatic effect of PLX4720 was lost in mice depleted of NK cells even at a lower dose of LWT1 tumor cells (Supplementary Fig. S2). These results demonstrated that the antimetastatic effects of PLX4720 relied not only on the intrinsic inhibition of melanoma cell proliferation, but also required the action of host NK cells.

Antimetastatic effect of PLX4720 depends on NK cell-mediated cytotoxicity

We next evaluated the importance of effector pathways in PLX4720-driven NK cell-mediated control of LWT1 lung metastasis. We observed that PLX4720 was still effective in mice neutralized for IFN γ or in mice deficient for IFN γ ($^{-/-}$), suggesting that the IFN γ pathway was not required for PLX4720 efficacy *in vivo* in this mouse tumor model (Fig. 3A). In contrast, mice deficient in perforin (*Pfp* $^{-/-}$) alone or additionally neutralized for IFN γ were unable to control LWT1 metastasis when treated with PLX4720 (Fig. 3A). These results suggested that in the LWT1 tumor model, perforin played a major role in controlling the antimetastatic efficacy of PLX4720.

NK cell release of cytotoxic granules is controlled by the integration of signals received by a wide set of activation and inhibitory receptors (23, 24). We could not detect Rae-1 family ligands while CD155 was highly expressed on LWT1 cells (Fig. 3B). In contrast, the expression of MHC-I molecules H2-K^b and H2D^b was low at the cell surface of LWT1 cells (Fig. 3B). In

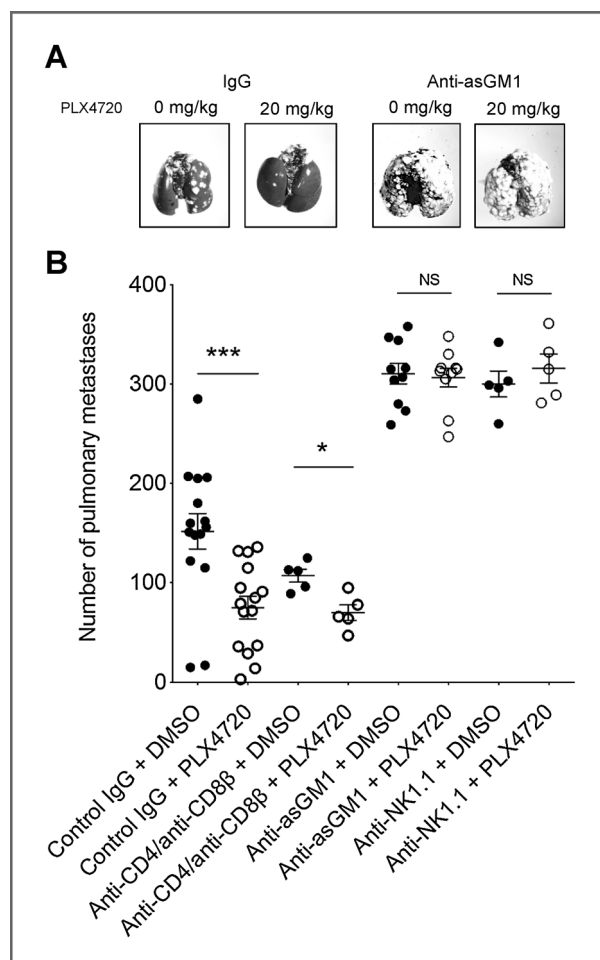


Figure 2. Antimetastatic effects of PLX4720 require NK cells. C57BL/6 WT mice were injected with the indicated depleting antibodies and were challenged intravenously with 5×10^5 LWT1 melanoma cells. Mice were subsequently treated with 20 mg/kg or equivalent amount of DMSO daily from day 1 to 7. After 14 days, lungs were harvested and perfused with India ink and lung metastases were counted under a microscope. A, representative pictures of lungs from the indicated group of mice. B, graph representing the mean \pm SEM numbers of lung metastases in the indicated group of mice. Pooled data from two independent experiments are shown. Each symbol represents one individual mouse. NS, nonsignificant, $P > 0.05$; *, $P < 0.05$; ***, $P < 0.001$ Mann-Whitney test.

accordance with the low density of MHC-I and the presence of CD226 ligands, we found that LWT1 was well killed by activated NK cells in 4-hour classical ^{51}Cr assays (Fig. 3C). Interestingly, the presence of anti-CD226 antibodies in the assay was able to limit LWT1 killing, suggesting that the CD226 interaction with CD155 is important for NK cell recognition of LWT1 (Fig. 3C).

Therefore, using gene-targeted mice for CD226 (*Cd226* $^{-/-}$), we tested the role of these receptors in PLX4720-driven NK cell-mediated control of LWT1 lung metastasis. We found that the effect of PLX4720 was partially compromised in *Cd226* $^{-/-}$ mice (Fig. 3D). Additional neutralization of NKG2D did not further abrogate the activity of PLX4720 (Fig. 3D). Altogether, our

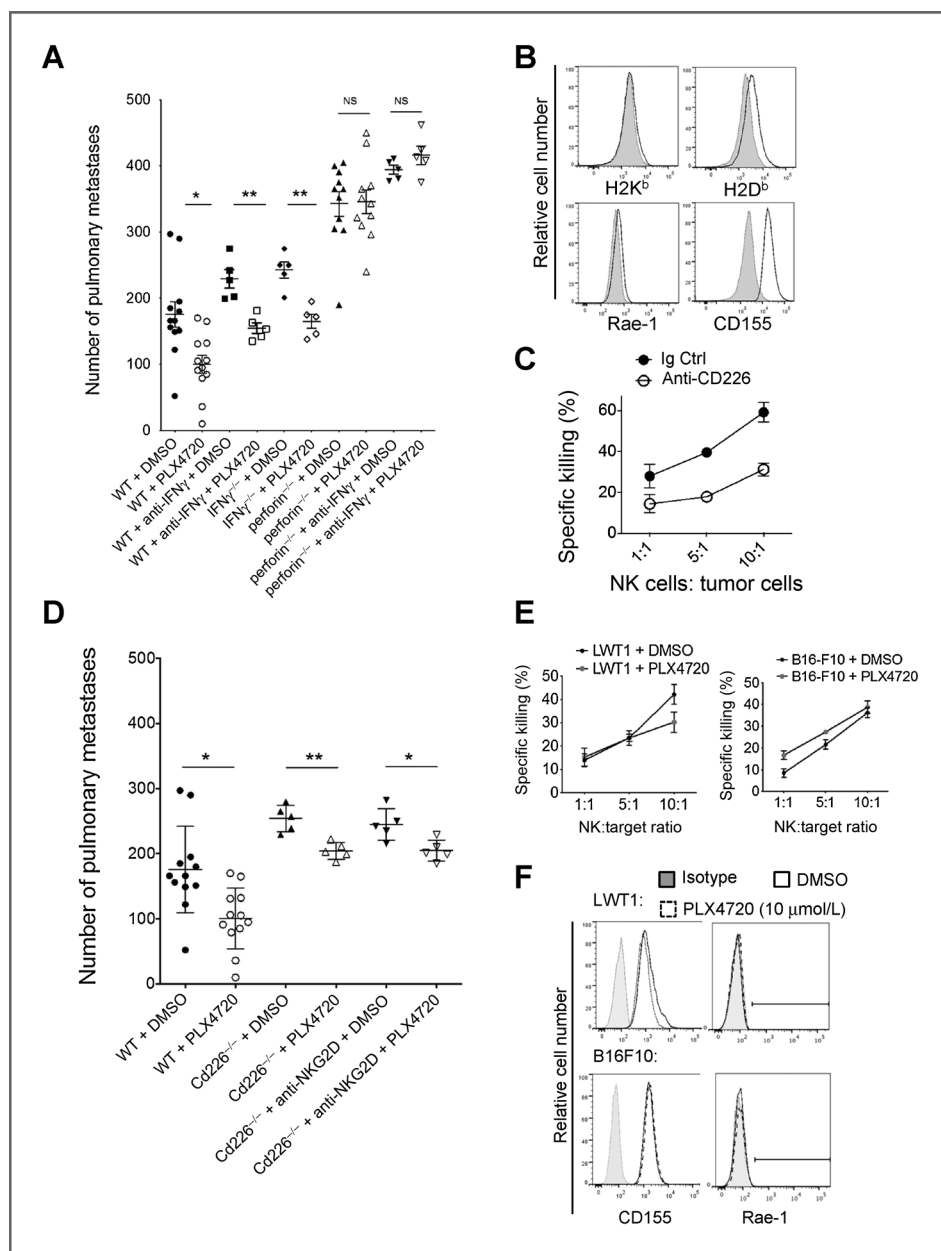
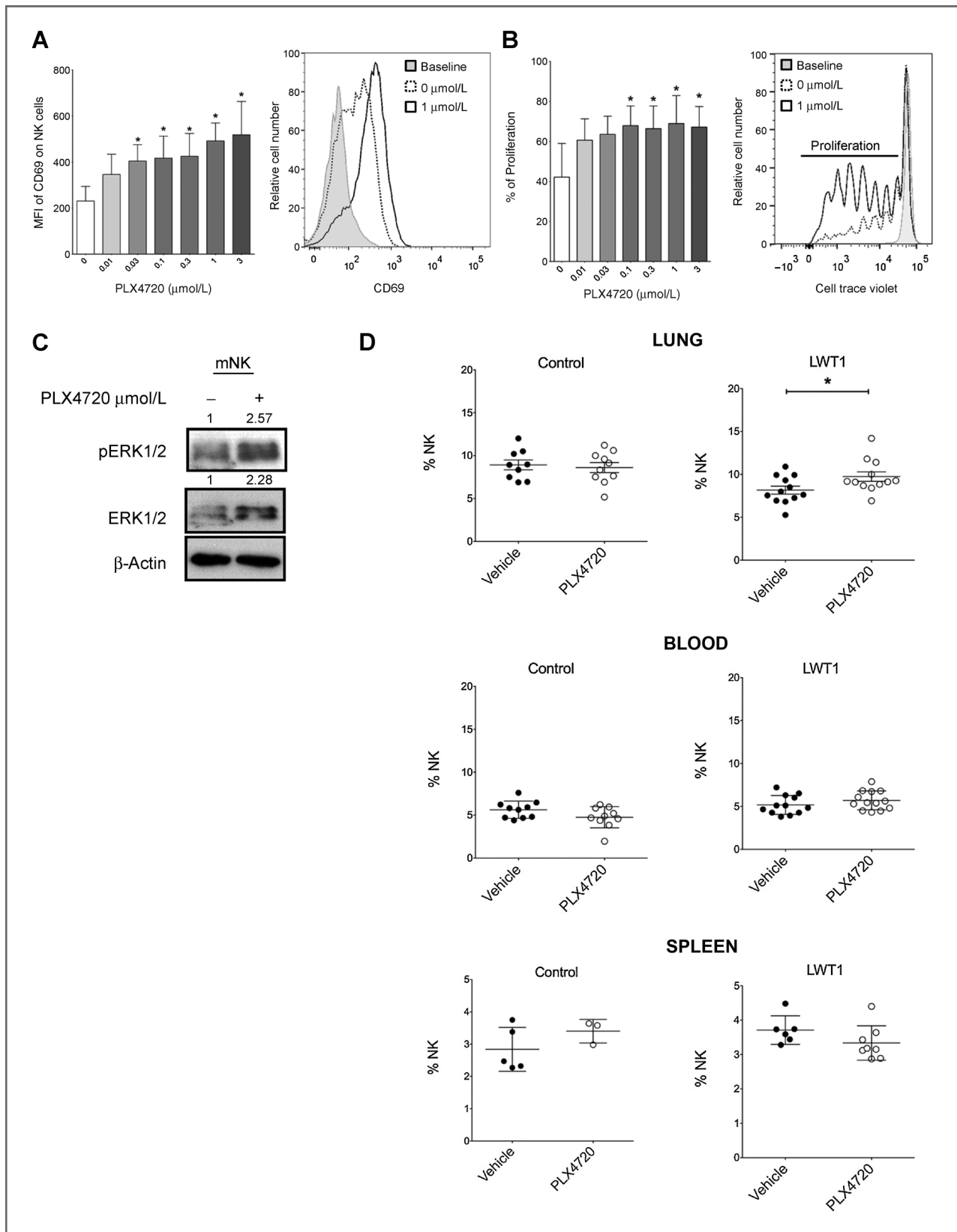


Figure 3. PLX4720 requires perforin and CD226 for optimal antimetastatic activity. **A** and **D**, the indicated strains of mice were challenged intravenously with 5×10^5 LWT1 melanoma cells and subsequently treated with 20 mg/kg or equivalent amount of DMSO daily on days 1 to 7. Antibody neutralization was performed on days -1, 0, and 7 relative to tumor challenge. After 14 days, lungs were perfused with India ink and metastases were counted under a microscope. **A** and **D**, the mean \pm SEM number of lung metastases in the indicated groups of mice are shown. Data are pooled from two independent experiments. Each symbol represents an individual mouse. **B**, LWT1 cells were stained with antibodies against the indicated extracellular proteins and analyzed by flow cytometry. The gray histograms represent isotype controls, whereas the black lines represent the test staining. **C**, LWT1 cells were ⁵¹Cr-labeled followed by 4 hours of coculture with activated NK cells in the presence of Ig control or anti-CD226 antibodies. Graph represents the mean \pm SD of experimental replicates. Data are representative of three independent experiments. **E** and **F**, LWT1 and B16F10 cells were treated *in vitro* with 10 μ mol/L of PLX4720 or equivalent amount of DMSO for 24 hours. Cells were either labeled ⁵¹Cr and used as target in a cytotoxicity assay (**E**) or analyzed by flow cytometry for Rae-1 and CD155 expression (**F**). **E**, NK cells were activated *in vitro* for 48 hours with media supplemented with 10 ng/mL IL15/IL15R α followed by 4 hours of incubation with PLX4720 or DMSO-treated B16F10 or LWT1 cells. Data are representative of three independent experiments. Graphs show mean \pm SD of three experimental replicates. NS $P > 0.05$; *, $P < 0.05$; **, $P < 0.01$; Mann-Whitney test.

results show that the antimetastatic effects of PLX4720 require both perforin-mediated cytotoxicity and in part, tumor recognition via CD226.

To test whether PLX treatment of tumor cells increased LWT1 sensitivity to NK cell-mediated killing, LWT1 or B16F10 was cultured *in vitro* in the presence of 10 μ mol/L of PLX4720



or DMSO for 24 hours. We found that PLX4720 pretreatment of these target cells neither affected the NK cell-mediated killing of BRAF^{V600E} nor BRAF^{wt} tumor cells (Fig. 3E). Consistent with these findings, the expression levels of Rae-1, CD155, and MHC class I molecules were not affected by BRAF inhibition (Fig. 3F).

PLX4720 directly impacts mouse NK cells

We next tested freshly purified NK cells activated with IL2 in the presence of increasing concentrations of PLX4720. Supplementation with PLX4720 significantly increased NK cell CD69 (Fig. 4A) and NK cell proliferation (Fig. 4B). In contrast, we did not observe any impact of PLX4720 on IFN γ production by NK cells in response to IL12 and IL18 cytokine combinations (Supplementary Fig. S3) or PLX4720 on NK cell-mediated cytotoxicity induced by IL15 (Supplementary Fig. S4). PLX4720 has been shown to increase ERK1/2 phosphorylation in BRAF^{wt} cells (21, 22). We observed an increase in ERK1/2 phosphorylation after 24-hour PLX4720 treatment and an increase in total ERK1/2 expression after PLX4720 treatment, while β -actin levels were not modulated (Fig. 4C). PLX4720 also displayed NK cell modulatory functions *in vivo* because C57BL/6 mice bearing LWT1 lung metastases and treated with PLX4720 (20 mg/kg daily) for 24 hours had an increased NK cell frequency in the lungs compared with DMSO-treated mice or mice that had not been inoculated intravenously with LWT1 melanoma (Fig. 4D).

PLX4720 and IL2 combination therapy suppresses melanoma metastasis

Given the demonstrated effects of PLX4720 and IL2 on NK cell proliferation *ex vivo* and the important role of NK cells in PLX4720 mechanism of action *in vivo*, we next assessed whether a combination of PLX4720 and IL2 could combine to suppress LWT1 metastasis in mice. We have previously shown the antitumor activity of IL2 in other models of tumor metastasis in mice (25) and herein used a similar dose/regimen of daily IL2 for 5 days concurrent with PLX4720 treatment. Notably, mice receiving a combination of PLX4720 and IL2 displayed significantly lower levels of LWT1 pulmonary metastasis compared with mice treated with either agent alone or DMSO/PBS (Fig. 5). Because IL2 has been standardly used in the treatment of advanced human malignant melanoma (26), these data suggest that this combination should now be further explored in this preclinical model.

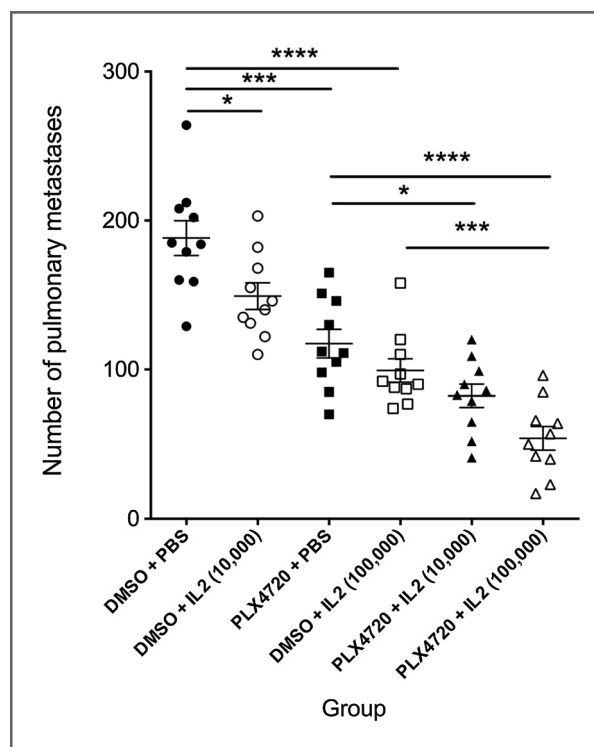


Figure 5. IL2 enhances the antimetastatic activity of PLX4720. A total of 5×10^5 LWT1 melanoma cells were injected i.v. into C57BL/6 WT mice and mice were subsequently treated with 20 mg/kg or equivalent amount of DMSO daily on days 1 to 7 and/or PBS or the indicated amount of IL2 (10,000 U or 100,000 U i.p.) given daily on days 1 to 5. Mice were sacrificed on day 14 and lungs harvested and fixed as described in Materials and Methods. Data are from two pooled experiments, with graphs representing the mean \pm SEM pulmonary colonies of each group of five mice. Statistical analysis by Mann-Whitney test (*, $P < 0.05$; ***, $P < 0.001$; ****, $P < 0.0001$).

PLX4720 and IL2 increase human NK cell functions

Finally, to determine whether a similar mechanism may occur in PLX4720-treated cancer patients, we investigated whether PLX4720 directly impacted human NK cells. We observed a clear increase in ERK1/2 phosphorylation after PLX4720 treatment for 24 hours (Fig. 6A). Interestingly, like in mouse NK cells, an increase in total ERK1/2 was associated with PLX4720 treatment, whereas β -actin expression remained comparable between the two groups of NK cells (Fig. 6A). We next cultured NK cells for 6 days with IL2 and

Figure 4. PLX4720 enhances NK cell activation and proliferation. A and B, Cell Trace Violet-labeled purified NK cells were cultured with the indicated doses of PLX4720 in media supplemented with 300 U/mL IL2. Analysis of CD69 and proliferation was performed by flow cytometry. A, the mean \pm SD CD69 expression of triplicates (left) and representative histograms showing CD69 expression (right) are shown. B, the mean \pm SD percentage of divided NK cells (left) and representative histograms showing Cell Trace Violet dilution (right) after 3 days in culture are shown. A and B, data are representative of three independent experiments. Statistical analysis performed by unpaired Student *t* test, *, $P < 0.05$. C, 2×10^6 purified NK cells were cultured for 24 hours in the presence of PLX4720 or DMSO in media supplemented with 300 U/mL IL2. The phosphorylation of ERK1/2 and the total amount of ERK1/2 and β -actin were measured in cell lysate by Western blot analysis. Fold increase relative to no PLX4720 control is recorded above the lane. Representative images of three independent experiments are shown. D, naïve C57BL/6 WT mice (control) or C57BL/6 WT mice injected i.v. with 5×10^5 LWT1 melanoma cells (LWT1) were treated i.p. with 20 mg/kg PLX4720 or an equivalent amount of DMSO (vehicle) for 24 hours. Twenty-four hours after this treatment, mice were sacrificed and frequencies of NK cells in the lungs, peripheral blood, and spleens were determined by flow cytometry. The mean \pm SEM percentages of NK cells are shown. Data pooled from two independent experiments are shown. *, $P < 0.05$ Mann-Whitney test.

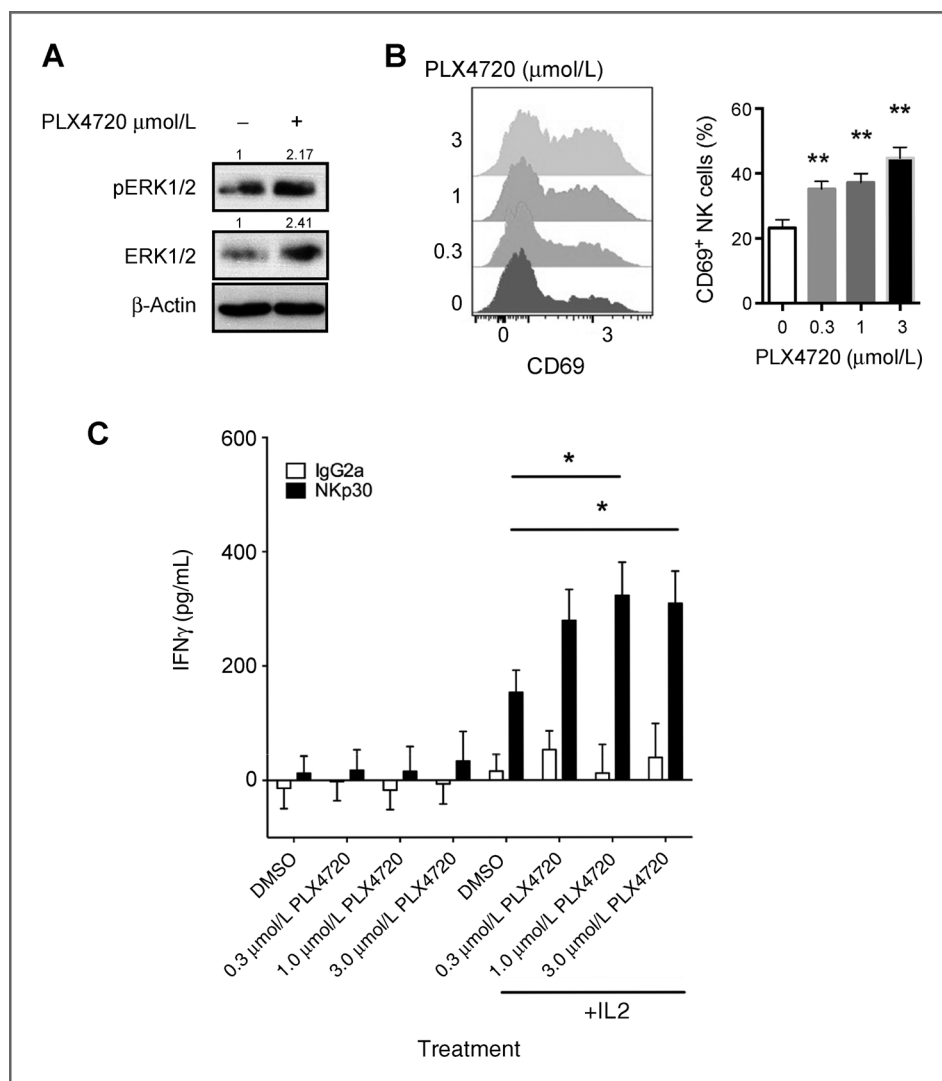


Figure 6. PLX4720 enhances human NK cell activation. **A**, 2×10^6 human NK cells purified from PBMC of healthy donors were cultured for 24 hours in the presence of PLX4720 or DMSO in media supplemented with 300 U/mL IL2. The phosphorylation of ERK1/2, the total amount of ERK1/2 and β -actin were measured in cell lysate by Western blot analysis. Fold increase relative to no PLX4720 control is recorded above the lane. Representative images of two independent experiments are shown. **B**, purified human NK cells were cultured with the indicated doses of PLX4720 in media supplemented with 300 U/mL IL2. The representative histograms showing CD69 expression (left) and the mean \pm SD CD69 expression of experimental replicates (right) are shown. Data are representative of four independent healthy donors. Statistical analysis was performed by unpaired Student *t* test, **, $P < 0.01$. **C**, purified human NK cells from nine donors were cultured in DMSO or PLX4720 (0.3–3.0 μ mol/L as indicated) with or without IL2 (300 U/mL) for 20 hours. NK cells were then plated (5×10^4 /well) in wells coated with anti-NKp30 (\pm IL2 1,000 U/mL) and incubated for an additional 20 hours. Supernatants were harvested and IFN γ released in the supernatant measured by ELISA. Statistical analysis performed by Mann-Whitney test as indicated (*, $P < 0.05$).

increasing concentrations of PLX4720. We observed that PLX4720 induced a dose-dependent increase in CD69 expression on NK cells, demonstrating that PLX4720 potentiates human NK cell activation induced by IL2 (Fig. 6B). Finally, human NK cells secrete IFN γ when ligated via NKp30 in the context of IL2 activation (27). We assessed the effect of PLX4720 on NKp30/IL2-induced IFN γ secretion by purified NK cells from 9 different human donors. We observed that increasing concentrations of PLX (0.3 to 3 μ mol/L) significantly enhanced the level of IFN γ above IL2 or NKp30 triggering alone (Fig. 6C). In contrast, PLX was unable to enhance the IFN γ secreted from human NK cells exposed to IL12/IL18 (data not shown).

Discussion

Because of the lack of a mouse model, the mechanisms involved in the control of metastatic melanoma by BRAF^{V600E} inhibitor has remained until now, unknown. In this study using a syngeneic BRAF^{V600E} metastatic melanoma mouse

model in immune-competent mice, we demonstrated that the antimetastatic effects of a selective BRAF^{V600E} inhibitor PLX4720 require the action of host NK cells and perforin, and in part, the recognition/adhesion molecule, CD226. We showed that PLX4720 increases the phosphorylation of ERK1/2, CD69 expression, and proliferation of mouse NK cells *in vitro*. NK cell frequencies were significantly enhanced by PLX4720 specifically in the lungs of mice with BRAF^{V600E} lung metastases. Furthermore, PLX4720 also increased human NK cell pERK1/2, CD69 expression, and IFN γ release in the context of anti-NKp30/IL2 stimulation. Finally, we demonstrated that therapy with a low or high dose of IL2 combined with PLX4720 was able to limit metastatic burden in mice. These findings revealed the importance of NK cells in treating BRAF^{V600E} metastatic melanoma and now provide the basis for additionally exploring the curative potential of BRAF^{V600E} inhibitors in combination with immunotherapies that engage NK cells.

Many reports have highlighted the importance of NK cells for immunotherapy, such as dendritic cell-based

immunotherapy (28), IFN α and IL2 (29, 30). Now we can consider that BRAF^{V600E} inhibitors may exert a large part of their antimetastatic activity via NK cells. Furthermore, the safety and efficacy of vemurafenib combined with IFN α -2b is currently under investigation in a new clinical trial (ClinicalTrials.gov identifier NCT01943422), although the study is reportedly not recruiting yet. IFN α 2b is an adjuvant treatment for patients with resected stage III melanoma, known to upregulate the expression of MHC class I on tumor cells, therefore increasing tumor antigenicity for recognition by CD8⁺ T cells (31). Although engaging CD8⁺ T cells is generally a positive approach to therapy, the recognition of MHC class I by NK cells triggers inhibitory signaling to reduce NK cell-mediated cytotoxicity and IFN γ production (23). Because here we found that the antimetastatic effects of PLX4720 require NK cells, it is possible that the upregulation of MHC class I on BRAF^{V600E}-mutant melanoma by IFN α 2b might also impair the NK cell-related antimetastatic effects of the BRAF inhibitor, vemurafenib. The enhanced antimetastatic activity of low-dose IL2 and PLX4720 in this model of BRAF^{V600E}-mutant melanoma encourages us to explore other means to improve the NK cell-mediated control of metastasis in humans with BRAF^{V600E}-mutant melanoma. IL21 has shown promise in the treatment of malignant melanoma (32) and has antimetastatic activity and can terminally differentiate NK cells (33). Antibodies reactive with KIR, that relieve MHC class I inhibition, have also been shown to promote NK cell antitumor activity (34). Combinations of these agents with BRAF inhibitors in the treatment of melanoma are now worthy of further exploration.

Although cutaneous melanoma can be treated by surgical excision with great effectiveness when diagnosed early, metastasis of such tumors remains incurable (35). Therefore, investigation of strategies that eliminate remaining or resistant tumor cells is urgently needed. Once it was clear that NK cells were critical in controlling pulmonary metastasis of LWT1, we then tested whether NK cells were necessary for the antimetastatic activity of PLX4720. This was of important, because BRAF^{V600E} inhibitors have mostly been examined in immune-deficient SCID mice that lack T and B cells, but do have NK cells (4). Here, we showed that the depletion of NK cells completely abolished the antimetastatic effects of PLX4720 treatment. We directly demonstrated *ex vivo* the enhancement of mouse NK cell pERK and CD69 expression, and proliferation by the BRAF^{V600E} inhibitor in the context of IL2 culture. Human NK cell cultures revealed similar pERK1/2 and CD69 upregulation and an increase in IFN γ release by NK cells triggered via the activation receptor, NKp30, in the context of IL2. PLX4720 possibly increases ERK1/2 phosphorylation in BRAF WT cells (like NK cells) by a previously described mechanism (21, 22), whereas ATP-competitive inhibitors increase pERK1/2 levels by inhibiting CRAF inhibitory

autophosphorylation, thereby activating the RAF and MAPK pathways.

Follow-up studies should now be performed on peripheral blood and other samples from human cancer patients receiving BRAF inhibitors to determine whether NK cell proliferation and effector functions are being regulated by treatment and how durable or transient these changes might be. It is possible that BRAF inhibitors may have a slightly different spectrum of activities on human NK cells to those observed in mouse NK cells and caution must be taken in translating observations from the mouse to humans. Furthermore, patients with melanoma are now receiving BRAF inhibitor and MEK inhibitor in combination and we might predict that this combination might abrogate any activation of BRAF WT NK cells. Thus far, the clinical focus has been to try and improve the curative potential of BRAF^{V600E} inhibitors by combination with T-cell checkpoint inhibitors, such as anti-CTLA-4 or anti-PD-1. These combination approaches have surprisingly revealed some new toxicities (36). In contrast, therapies that attempt to improve the antimetastatic activities of BRAF^{V600E} inhibitors by promoting NK cell function have not been rationally explored in the clinic. These approaches may improve overall survival in patients receiving BRAF inhibitors.

Disclosure of Potential Conflicts of Interest

No potential conflicts of interest were disclosed.

Authors' Contributions

Conception and design: L. Ferrari de Andrade, S.F. Ngiow, L. Martinet, M.J. Smyth

Development of methodology: L. Ferrari de Andrade, L. Martinet

Acquisition of data (provided animals, acquired and managed patients, provided facilities, etc.): L. Ferrari de Andrade, S.F. Ngiow, K. Stannard, S. Rusakiewicz, M. Kalimutho, S.-K. Tey, L. Zitvogel, L. Martinet, M.J. Smyth

Analysis and interpretation of data (e.g., statistical analysis, biostatistics, computational analysis): L. Ferrari de Andrade, S.F. Ngiow, S. Rusakiewicz, M.J. Smyth

Writing, review, and/or revision of the manuscript: L. Ferrari de Andrade, S.F. Ngiow, K.K. Khanna, L. Martinet, M.J. Smyth

Administrative, technical, or material support (i.e., reporting or organizing data, constructing databases): K. Takeda

Study supervision: S.F. Ngiow, K.K. Khanna, M.J. Smyth

Acknowledgments

The authors thank Kate Elder and Liam Town for the care, maintenance, and genotyping of the mouse colonies.

Grant Support

L. Ferrari de Andrade was supported by a Conselho Nacional de Desenvolvimento Científico e Tecnológico (CNPq) scholarship and M.J. Smyth was supported by a National Health and Medical Research Council of Australia (NH&MRC) Australia Fellowship and NH&MRC Program Grant.

The costs of publication of this article were defrayed in part by the payment of page charges. This article must therefore be hereby marked *advertisement* in accordance with 18 U.S.C. Section 1734 solely to indicate this fact.

Received May 6, 2014; revised September 25, 2014; accepted October 9, 2014; published OnlineFirst October 28, 2014.

References

1. Siegel R, Ma J, Zou Z, Jemal A. Cancer statistics, 2014. *CA* 2014; 64:9–29.
2. Davies H, Bignell GR, Cox C, Stephens P, Edkins S, Clegg S, et al. Mutations of the BRAF gene in human cancer. *Nature* 2002;417:949–54.

3. Sosman JA, Kim KB, Schuchter L, Gonzalez R, Pavlick AC, Weber JS, et al. Survival in BRAF V600-mutant advanced melanoma treated with vemurafenib. *N Engl J Med* 2012;366:707–14.
4. Tsai J, Lee JT, Wang W, Zhang J, Cho H, Mamo S, et al. Discovery of a selective inhibitor of oncogenic B-Raf kinase with potent antimelanoma activity. *Proc Natl Acad Sci U S A* 2008;105:3041–6.
5. Joseph EW, Pratilas CA, Poulidakos PI, Tadi M, Wang W, Taylor BS, et al. The RAF inhibitor PLX4032 inhibits ERK signaling and tumor cell proliferation in a V600E BRAF-selective manner. *Proc Natl Acad Sci U S A* 2010;107:14903–8.
6. Chapman PB, Hauschild A, Robert C, Haanen JB, Ascierto P, Larkin J, et al. Improved survival with vemurafenib in melanoma with BRAF V600E mutation. *N Engl J Med* 2011;364:2507–16.
7. Flaherty KT, Puzanov I, Kim KB, Ribas A, McArthur GA, Sosman JA, et al. Inhibition of mutated, activated BRAF in metastatic melanoma. *N Engl J Med* 2010;363:809–19.
8. Nazarian R, Shi H, Wang Q, Kong X, Koya RC, Lee H, et al. Melanomas acquire resistance to B-RAF(V600E) inhibition by RTK or N-RAS upregulation. *Nature* 2010;468:973–7.
9. Villanueva J, Vultur A, Lee JT, Somasundaram R, Fukunaga-Kalabis M, Cipolla AK, et al. Acquired resistance to BRAF inhibitors mediated by a RAF kinase switch in melanoma can be overcome by cotargeting MEK and IGF-1R/PI3K. *Cancer Cell* 2010;18:683–95.
10. Sumimoto H, Imabayashi F, Iwata T, Kawakami Y. The BRAF-MAPK signaling pathway is essential for cancer-immune evasion in human melanoma cells. *J Exp Med* 2006;203:1651–6.
11. Knight DA, Ngjow SF, Li M, Parmenter T, Mok S, Cass A, et al. Host immunity contributes to the anti-melanoma activity of BRAF inhibitors. *J Clin Invest* 2013;123:1371–81.
12. Frederick DT, Piris A, Cogdill AP, Cooper ZA, Lezcano C, Ferrone CR, et al. BRAF inhibition is associated with enhanced melanoma antigen expression and a more favorable tumor microenvironment in patients with metastatic melanoma. *Clin Cancer Res* 2013;19:1225–31.
13. Wilmott JS, Long GV, Howle JR, Haydu LE, Sharma RN, Thompson JF, et al. Selective BRAF inhibitors induce marked T-cell infiltration into human metastatic melanoma. *Clin Cancer Res* 2012;18:1386–94.
14. Liu C, Peng W, Xu C, Lou Y, Zhang M, Wargo JA, et al. BRAF inhibition increases tumor infiltration by T cells and enhances the antitumor activity of adoptive immunotherapy in mice. *Clin Cancer Res* 2013;19:393–403.
15. Khalili JS, Liu S, Rodriguez-Cruz TG, Whittington M, Wardell S, Liu C, et al. Oncogenic BRAF(V600E) promotes stromal cell-mediated immunosuppression via induction of interleukin-1 in melanoma. *Clin Cancer Res* 2012;18:5329–40.
16. Boni A, Cogdill AP, Dang P, Udayakumar D, Njauw CN, Sloss CM, et al. Selective BRAFV600E inhibition enhances T-cell recognition of melanoma without affecting lymphocyte function. *Cancer Res* 2010;70:5213–9.
17. Ngjow SF, Knight DA, Ribas A, McArthur GA, Smyth MJ. BRAF-targeted therapy and immune responses to melanoma. *Oncoimmunology* 2013;2:e24462.
18. Devaud C, Westwood JA, John LB, Flynn JK, Paquet-Fifield S, Duong CP, et al. Tissues in different anatomical sites can sculpt and vary the tumor microenvironment to affect responses to therapy. *Mol Ther* 2014;22:18–27.
19. Straussman R, Morikawa T, Shee K, Barzily-Rokni M, Qian ZR, Du J, et al. Tumour micro-environment elicits innate resistance to RAF inhibitors through HGF secretion. *Nature* 2012;487:500–4.
20. Goel VK, Ibrahim N, Jiang G, Singhal M, Fee S, Flotte T, et al. Melanocytic nevus-like hyperplasia and melanoma in transgenic BRAFV600E mice. *Oncogene* 2009;28:2289–98.
21. Holderfield M, Merritt H, Chan J, Wallroth M, Tandeske L, Zhai H, et al. RAF inhibitors activate the MAPK pathway by relieving inhibitory autophosphorylation. *Cancer Cell* 2013;23:594–602.
22. Poulidakos PI, Zhang C, Bollag G, Shokat KM, Rosen N. RAF inhibitors transactivate RAF dimers and ERK signalling in cells with wild-type BRAF. *Nature* 2010;464:427–30.
23. Long EO, Kim HS, Liu D, Peterson ME, Rajagopalan S. Controlling natural killer cell responses: integration of signals for activation and inhibition. *Annu Rev Immunol* 2013;31:227–58.
24. Chan CJ, Smyth MJ, Martinet L. Molecular mechanisms of natural killer cell activation in response to cellular stress. *Cell Death Differ* 2014;21:5–14.
25. Teng MW, von Scheidt B, Duret H, Towne JE, Smyth MJ. Anti-IL-23 monoclonal antibody synergizes in combination with targeted therapies or IL-2 to suppress tumor growth and metastases. *Cancer Res* 2011;71:2077–86.
26. Rosenberg SA. Raising the bar: the curative potential of human cancer immunotherapy. *Sci Transl Med* 2012;4:127ps8.
27. Delahaye NF, Rusakiewicz S, Martins I, Ménard C, Roux S, Lyonnet L, et al. Alternatively spliced NKp30 isoforms affect the prognosis of gastrointestinal stromal tumors. *Nat Med* 2011;17:700–7.
28. Bouwer AL, Saunderson SC, Caldwell FJ, Damani TT, Pelham SJ, Dunn AC, et al. NK cells are required for dendritic cell-based immunotherapy at the time of tumor challenge. *J Immunol* 2014;192:2514–21.
29. Johnston SR, Constenla DO, Moore J, Atkinson H, A'Hern RP, Dadian G, et al. Randomized phase II trial of BCDT [carmustine (BCNU), cisplatin, dacarbazine (DTIC) and tamoxifen] with or without interferon alpha (IFN-alpha) and interleukin (IL-2) in patients with metastatic melanoma. *Br J Cancer* 1998;77:1280–6.
30. Konjevic G, Jovic V, Jurisic V, Radulovic S, Jelic S, Spuzic I. IL-2-mediated augmentation of NK-cell activity and activation antigen expression on NK- and T-cell subsets in patients with metastatic melanoma treated with interferon-alpha and DTIC. *Clin Exp Metastasis* 2003;20:647–55.
31. Di Trollo R, Simeone E, Di Lorenzo G, Grimaldi AM, Romano A, Ayala F, et al. Update on PEG-interferon alpha-2b as adjuvant therapy in melanoma. *Anticancer Res* 2012;32:3901–9.
32. Davis ID, Brady B, Kefford RF, Millward M, Cebon J, Skrumsager BK, et al. Clinical and biological efficacy of recombinant human interleukin-21 in patients with stage IV malignant melanoma without prior treatment: a phase IIa trial. *Clin Cancer Res* 2009;15:2123–9.
33. Brady J, Hayakawa Y, Smyth MJ, Nutt SL. IL-21 induces the functional maturation of murine NK cells. *J Immunol* 2004;172:2048–58.
34. Thielens A, Vivier E, Romagne F. NK cell MHC class I specific receptors (KIR): from biology to clinical intervention. *Curr Opin Immunol* 2012;24:239–45.
35. Tsao H, Atkins MB, Sober AJ. Management of cutaneous melanoma. *N Engl J Med* 2004;351:998–1012.
36. Johnson DB, Wallender EK, Cohen DN, Likhari SS, Zwerner JP, Powers JG, et al. Severe cutaneous and neurologic toxicity in melanoma patients during vemurafenib administration following anti-PD-1 therapy. *Cancer Immunol Res* 2013;1:373.

Cancer Research

The Journal of Cancer Research (1916–1930) | The American Journal of Cancer (1931–1940)

Natural Killer Cells Are Essential for the Ability of BRAF Inhibitors to Control BRAF^{V600E}-Mutant Metastatic Melanoma

Lucas Ferrari de Andrade, Shin F. Ngjow, Kimberley Stannard, et al.

Cancer Res 2014;74:7298-7308. Published OnlineFirst October 28, 2014.

Updated version Access the most recent version of this article at:
doi:[10.1158/0008-5472.CAN-14-1339](https://doi.org/10.1158/0008-5472.CAN-14-1339)

Supplementary Material Access the most recent supplemental material at:
<http://cancerres.aacrjournals.org/content/suppl/2014/10/28/0008-5472.CAN-14-1339.DC1.html>

Cited articles This article cites 36 articles, 15 of which you can access for free at:
<http://cancerres.aacrjournals.org/content/74/24/7298.full.html#ref-list-1>

E-mail alerts [Sign up to receive free email-alerts](#) related to this article or journal.

Reprints and Subscriptions To order reprints of this article or to subscribe to the journal, contact the AACR Publications Department at pubs@aacr.org.

Permissions To request permission to re-use all or part of this article, contact the AACR Publications Department at permissions@aacr.org.